Effects of Exogenous Proteins on Cytoplasmic Streaming in Perfused *Chara* Cells

EUGENE A. NOTHNAGEL, JOSEPH W. SANGER, and W. W. WEBB
School of Applied and Engineering Physics, Cornell University, Ithaca, New York 14853; and Department of Anatomy, School of Medicine, University of Pennsylvania, Philadelphia, Pennsylvania 19174. Dr. Nothnagel's present address is Department of Chemistry, University of Colorado, Boulder, Colorado 80309

ABSTRACT Cytoplasmic streaming in characean algae is thought to be generated by interaction between subcortical actin bundles and endoplasmic myosin. Most of the existing evidence supporting this hypothesis is of a structural rather than functional nature. To obtain evidence bearing on the possible function of actin and myosin in streaming, we used perfusion techniques to introduce a number of contractile and related proteins into the cytoplasm of streaming *Chara* cells. Exogenous actin added at concentrations as low as 0.1 mg/ml is a potent inhibitor of streaming. Deoxyribonuclease I (DNase I), an inhibitor of amoeboid movement and fast axonal transport, does not inhibit streaming in *Chara*. Fluorescein-DNase I stains stress cables and microfilaments in mammalian cells but does not bind to *Chara* actin bundles, thus suggesting that the lack of effect on streaming is due to a surprising lack of DNase I affinity for *Chara* actin bundles. Heavy meromyosin (HMM) does not inhibit streaming, but fluorescein-HMM (FL-HMM), having a partially disabled EDTA ATPase, does. Quantitative fluorescence micrography provides evidence that inhibition of streaming by FL-HMM may be due to a tendency for FL-HMM to remain bound to *Chara* actin bundles even in the presence of MgATP. Perfusion with various control proteins, including tubulin, ovalbumin, bovine serum albumin, and irrelevant antibodies, does not inhibit streaming. These results support the hypothesis that actin and myosin function to generate cytoplasmic streaming in *Chara*.

The central roles played by actin and myosin in the contraction of muscle have been firmly established. Although the presence of actin and myosin has been demonstrated in a wide variety of both plant and animal cells, the active involvement of these proteins in the generation of nonmuscle cell motility has not been demonstrated directly (1). Recent experiments have shown clearly that actin-myosin-containing stress fibers of fibroblastic cells are capable of contraction (2), yet even these observations do not establish that such contractions are essential for cell motility. It has been suggested that conclusive evidence for the involvement of actin and myosin in nonmuscle cell motility might come from experiments with cells having genetically defective actin or myosin (1). Until such mutants have been identified and characterized for a variety of organisms, less direct experiments can continue to provide valuable evidence on the question of actin-myosin involvement in nonmuscle cell motility. Use of cells that are both highly motile and readily manipulable facilitates such experiments.

The giant internodal cells of characean algae exhibit highly organized, rapid cytoplasmic streaming and, at the same time, can be subjected to a variety of mechanical and biochemical treatments without immediate stoppage of streaming. It is widely assumed that actin and myosin function together to produce streaming in these cells, although only limited direct evidence is available to support this assumption (3). The presence of actin-containing bundles attached to the chloroplast files at the interface between the stationary ectoplasm and moving endoplasm has been firmly established (4–7). The fact that these subcortical actin bundles are unidirectional (8) and are located at the site thought to be the seat of motive force (9) support the suggestion of an actin-myosin-based streaming mechanism. This hypothesis has been further supported by the observation of submicron-sized cytoplasmic particles which exhibit ATP-dependent (10) attachment to and motion along these bundles (11). Motile filaments long observed in cell-fragment preparations (12) have now been shown to contain actin and are probably fragments of the subcortical bundles (13). Biochemical extraction has verified the presence of a

THE JOURNAL OF CELL BIOLOGY · VOLUME 93 JUNE 1982 735–742

myosinlike molecule in the cells, although use of conventional muscle myosin extraction procedures produced very low yield (14). Ultrastructural studies have not revealed the presence of bipolar myosin filaments in *Chara* (15), although suggestive structures have been observed in association with membranous structures which may be derived from endoplasmic reticulum (15–17).

Proteins having well-characterized interactions with contractile proteins have found applications in the investigation of nonmuscle cell motility. Changes in motility observed after microinjection of such proteins suggest that the target proteins may be involved in force generation. Antibodies directed against contractile proteins have been used in several studies. Myosin antibody has been found to inhibit the cleavage of starfish blastomeres (18). Antibodies against tubulin (19) and dynein (20) altered the beating of sperm flagella. Deoxyribonuclease I (DNase I), known to depolymerize F-actin and form a tight 1:1 complex with G-actin (21), has also been used in motility studies. DNase I microinjection into *Amoeba* has been found to cause both inhibition of streaming and reduction of the actin filament system (22). DNase I (23, 24) and filamin (23) have been recently shown to inhibit axonal transport. These results have been interpreted as evidence for the role of actin filaments in amoeboid movement and axonal transport.

Microinjection of exogenous contractile proteins has also provided useful information on motile mechanisms, particularly when these proteins have been suitably modified. A variety of fluorescence-labeled proteins including actin, α-actinin, tropomyosin, and tubulin have been microinjected as probes of contractile protein localization and function in living cells (2, 25–27). Fluorescence labeling of these proteins has been carried out with the goal of retaining full biochemical activity so that the microinjected probes will likely mimic the location and function of the native cellular proteins (28). Other studies have used proteins modified so as to specifically disable part of the normal function. N-Ethylmaleimide-modified heavy meromyosin (NEM-HMM) binds to actin but does not release in the presence of MgATP (29). Thus NEM-HMM inhibits both contraction of muscle myofibrils and cell cleavage whereas unmodified heavy meromyosin (HMM) inhibits neither of these processes (29, 30). Interpretation of results obtained with exogenous proteins is not always obvious, however. Recent experiments have shown that contraction of glycerinated stress fibers is not inhibited by NEM-HMM, fluorescein isothiocyanate-(FITC)-HMM (FL-HMM), exogenous actin, or DNase I (2).

In an attempt to obtain additional evidence concerning the possible function of actin and myosin in streaming, we have perfused *Chara* cells with a variety of exogenous proteins including actin, HMM, DNase I, and tubulin. In some cases, we used fluorescence-labeled proteins to obtain information concerning the nature of action of these proteins. The results presented here show that both exogenous actin and FL-HMM produce dose-dependent inhibition of streaming. HMM, DNase I, tubulin, and a variety of control proteins do not inhibit streaming. These results are discussed in terms of the hypothesis that cytoplasmic streaming is generated by actin-myosin interactions. The results obtained with exogenous actin are relevant to the earlier conjecture (31) that concentrations of free endoplasmic actin are normally very low and that higher concentrations would inhibit streaming.

To the authors' knowledge, the only previous reports of effects of exogenous proteins on characean motility have involved endoplasmic drops or cell fragments. Kuroda and Kamiya (32) reported that chloroplast rotation in endoplasmic drops could be inhibited by N-ethylmaleimide and then partially reactivated by subsequent addition of HMM. Ishimura et al. (33) stated that p-chloromercuribenzoate-HMM inhibited chloroplast rotation, and Higashi-Fujime (13) stated that actin, myosin, HMM, and tropomyosin had no appreciable effect on movement of bundle fragments. No data or details were presented in these latter two reports.

MATERIALS AND METHODS

General

The growth and preparation of *Chara corallina* internodes, "window" formation, and the Tazawa (34) and Williamson (10) techniques of perfusion were done exactly as reported previously (31). Measurement of cytoplasmic streaming rates, fluorescence microscopy, photography, and microdensitometry were also as described (31). Growth, formaldehyde fixation, and staining of PtK_2 cells followed essentially the methods of Barak et al. (35).

Perfusion Buffers

We used several different perfusion buffers during the course of this study. Tazawa's perfusion fluid (TPF) (34) consisted of 30 mM HEPES, 5 mM EGTA, 6 mM $MgCl_2$, 1 mM Na_2ATP, 23.5 mM methanesulfonic acid, and 250 mM sorbitol. "TPF less ATP" consisted of TPF from which the 1 mM ATP had been deleted. "TPF with 0.1 mM ATP" was TPF containing 0.1 mM instead of 1 mM ATP. "TPF plus GTP" was TPF containing 1 mM Na_4GTP in addition to the 1 mM Na_2ATP. "TPF with 10 mM MgATP" consisted of 30 mM HEPES, 5 mM EGTA, 10 mM $MgCl_2$, 10 mM Na_2ATP, 23.5 mM methanesulfonic acid, and 210 mM sorbitol. All perfusion buffers were adjusted to pH 7.0 with KOH.

Proteins

Goat anti-rabbit IgG antiserum (IgG fraction abbreviated GAR), fluorescein-conjugated rabbit anti-goat IgG antiserum (IgG fraction abbreviated FL-RAG), and ovalbumin were obtained from United States Biochemical Corp., Cleveland, OH. Monomer standard bovine serum albumin (BSA) was obtained from Miles Laboratories, Inc. (Elkhart, IN). These proteins were dialyzed against the appropriate perfusion buffer and were used without further purification. Porcine brain tubulin was prepared and stored according to Crepeau et al. (36). Immediately before use, an aliquot of tubulin was thawed from liquid nitrogen and purified through two further cycles of warm/cold polymerization/depolymerization (36) using TPF plus GTP as the buffer.

Rabbit skeletal muscle actin was obtained from Worthington Biochemical Corp. (Freehold, NJ). SDS PAGE (37) showed that >90% of the protein appeared in a single band at apparent molecular weight 42,000, as expected. Impurities appeared principally in two bands corresponding to molecular weights 33,000 and 34,000. Actin to be used in perfusion experiments was purified through an additional cycle of polymerization/depolymerization as described (38). The final F-actin pellet was dissolved in buffer A (2 mM HEPES, 0.2 mM ATP, 0.2 mM $MgCl_2$, pH 8.0) and used as the stock solution.

Rabbit skeletal HMM and FL-HMM were prepared according to Sanger (39). Based on Lowry protein measurement (37) and an extinction coefficient of $6.8 \times 10^4\ M^{-1}\ cm^{-1}$ at 495 nm for bound fluorescein (25), the FL-HMM contained 7 mol of fluorescein per mole of HMM. Immediately before use FL-HMM was transferred to the desired buffer by gel filtration on Sephadex G-25.

Electrophoretically purified bovine pancreatic DNase I was obtained from Sigma Chemical Co. (St. Louis, MO). FITC-labeled DNase I (FL-DNase I) was prepared by a modification of the method used by Wang and Goldberg (40) for the preparation of rhodamine-labeled DNase I. To remove the glycine stabilizer added to DNase I by the manufacturer, 5 mg of DNase I were dissolved in 1.5 ml of 5 mM Na_2HPO_4, 1 mM $CaCl_2$, 0.5 mM $MgSO_4$, 50 mM NaCl, 0.1 mM phenylmethylsulfonyl fluoride, pH 7.5, and dialyzed overnight against several changes of the same buffer. An equal volume of 40 mM borate, 1 mM $CaCl_2$, 0.5 mM $MgSO_4$, 50 mM NaCl, pH 9.4, was then added together with 8 mg of 10% FITC on celite (Research Organics, Inc., Cleveland OH) to start fluorophore conjugation. The resulting suspension was mixed on a laboratory shaker for 30 min at 23°C. Celite was pelleted by centrifugation, and the colored supernatant was applied to a G-25 Sephadex column equilibrated with buffer B (20 mM imidazole-HCl, 5 mM $CaCl_2$, 2 mM $MgSO_4$, 20 mM NaCl, 1 mM NaN_3, pH 7.5). The column was developed with buffer B, and the colored fractions eluting in the void volume were pooled and applied to a DEAE-cellulose column equilibrated with buffer B. Unlabeled DNase I, which passed rapidly through the DEAE column under these conditions, was removed by washing the column with one to two column volumes of buffer B. FL-DNase I was then eluted from

the column by a linear 20–800 mM NaCl gradient in buffer B. Conjugates having low dye/protein ratio eluted early in the gradient and were found superior to higher conjugates which stained mammalian cells more intensely but also with increased nonspecific background. The FL-DNase I used for the experiments reported here contained 1.0 mol of fluorescein per mole of DNase I. Appropriate column fractions were pooled, concentrated, dialyzed against TPF less ATP, and stored frozen in liquid nitrogen.

Enzyme Assays

Unlabeled DNase I and FL-DNase I were assayed for nuclease activity according to Lindberg's standard spectrophotometric method (41). Nuclease activity in TPF less ATP or in TPF with 0.1 mM ATP was measured by this same technique with the indicated buffer substituted for the standard buffer (41). Inhibition of nuclease activity by actin was measured by the technique of Lazarides and Lindberg (42). All measurements were made at 23–24°C.

The ATPase rates of HMM and FL-HMM were determined by measuring the appearance of liberated phosphate (37). Calcium-ATPase activities were measured in 0.6 M KCl, 50 mM Tris-HCl, 10 mM $CaCl_2$, 5 mM Na_2ATP, pH 8.0. EDTA-ATPase activities were measured in 0.6 M KCl, 10 mM imidazole-HCl, 5 mM EDTA, 5 mM Na_2ATP, pH 7.2. All measurements were made at 23–24°C.

RESULTS

The perfusion technique of Tazawa et al. (34) was used to introduce proteins into the interior of streaming *Chara* cells. During this perfusion operation, which requires ~7 min to complete, only the vacuolar cell sap is replaced by the perfusion fluid. Within 10–20 min after perfusion, however, the EGTA in TPF causes dissolution of the tonoplast so that the contents of the vacuole and the endoplasm mix (31, 34). Hence if time is measured with $t = 0$ corresponding to the point of completion of the perfusion operation, then membrane-impermeable test substances (such as exogenous proteins) dissolved in the TPF will begin to enter the endoplasm at about $t = 10$ min. Effects of exogenous proteins on streaming may then be estimated by comparison with the time course of streaming in control cells perfused with TPF alone. The streaming rate in such control cells recovers to >50% of the preperfusion rate within 10 min after perfusion and then exhibits a slow decline with streaming continuing for >100 min (see references 31 and 34 and the closed-squares curve in Fig. 2). Since different cells show considerable variation in the persistence of streaming after perfusion (31), each curve presented here represents the average obtained from the number of trial perfusions indicated in the figure captions. Error bars representing standard deviations are drawn symmetrically about the data points.

Effect of Exogenous Actin on Streaming

Perfusion with TPF containing 0.1 mg/ml actin caused inhibition of streaming in *Chara* (Fig. 1). Inhibition became evident at ~10 min after perfusion and increased until 60 min at which time the streaming rate stabilized at ~10% of the preperfusion rate. When the concentration of actin in TPF was raised to 0.5 mg/ml, streaming in many cells stopped abruptly by 30 min after perfusion and in all cells was essentially 0 by 60 min (Fig. 1).

For comparison, control cells were perfused with TPF containing other proteins. The presence of 0.5 mg/ml tubulin in the TPF did not significantly alter streaming from that in cells perfused with TPF alone (Fig. 1, cf. closed-squares curve in Fig. 2). Streaming in cells perfused with a mixture of 0.25 mg/ml GAR and 0.25 mg/ml FL-RAG appeared to be slightly stabilized compared to streaming in the TPF and TPF plus tubulin controls (Fig. 1). This stabilization was most evident at longer times after perfusion with the streaming rate at 100 min still 50% of the preperfusion rate.

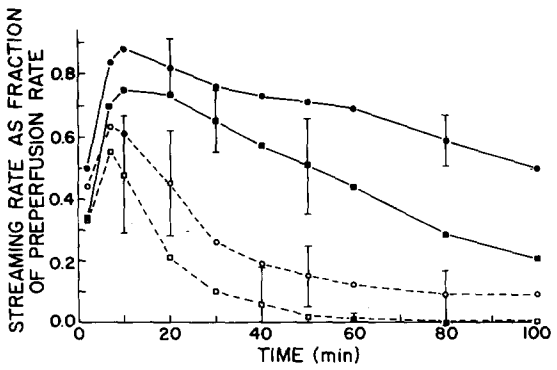

FIGURE 1 Effects on streaming of proteins applied intracellularly by Tazawa's (31, 34) perfusion technique. Perfusion was completed at $t = 0$ min. Cells were perfused with 0.1 mg/ml actin in TPF (open circles, average of four trials), 0.5 mg/ml actin in TPF (open squares, average of four trials), 0.5 mg/ml tubulin in TPF plus GTP (closed squares average of four trials), or 0.25 mg/ml GAR and 0.25 mg/ml FL-RAG in TPF (closed circles, average of four trials). Average preperfusion streaming rates were 95 (open circles), 88 (open squares), 93 (closed squares), and 66 μm/s (closed circles). Error bars are drawn symmetrically about the corresponding data points and represent standard deviations.

After cells are perfused with TPF, there is a slow decrease in not only the rate of streaming but also in the amount of streaming endoplasm (34). The streaming endoplasm in intact internodal cells forms a thin (≃10 μm thick) layer bounded by the ectoplasm toward the outside and by the tonoplast membrane toward the vacuole (3). After the tonoplast dissolves in perfused cells, the endoplasm is no longer bounded toward the vacuole and gradually dilutes into this region (34). Endoplasm in perfused cells also slowly accumulates at the tied ends of the cell. By action of these two processes, the amount of streaming endoplasm eventually reduces from the original 10-μm layer to small, micron-sized masses moving along the ectoplasm (34). In cells perfused with TPF alone, this decrease in amount of streaming endoplasm follows a time course roughly parallel to the decline in streaming rate.

In control cells perfused with tubulin or the mixed antibodies, the decrease in the amount of streaming endoplasm was not noticeably different from that in the TPF control cells. In cells perfused with actin, however, the amount of streaming endoplasm declined somewhat faster than in controls and was frequently accompanied by the appearance of one or more large (50–300 μm diameter) immobile aggregates of endoplasm in the vacuolar region (results not shown).

Effect of DNase I on Streaming

Streaming was not inhibited when cells were perfused with TPF containing 0.5 mg/ml DNase I. Compared to control cells perfused with TPF alone, streaming in DNase I-perfused cells was stabilized at times longer than 50 min (Fig. 2). The streaming rate at 100 min in DNase I-perfused cells was still >50% of the preperfusion rate.

As a control for this experiment, cells were perfused with 0.5 mg/ml BSA in TPF. Streaming in these control cells was also stabilized at times >50 min and was >50% of the preperfusion rate at 100 min (Fig. 2). There was no significant difference between streaming in cells perfused with 0.5 mg/ml DNase I and streaming in cells perfused with 0.5 mg/ml BSA. With either protein the amount of streaming endoplasm did not decline faster than in TPF control cells.

It is known that the nuclease activity of DNase I is at least 50 times greater in the presence of millimolar Ca^{++} with Mg^{++} than it is in the presence of Mg^{++} alone (41). To test whether Ca^{++} has a large effect on the DNase I-actin interaction, inhibition of DNase I activity by rabbit actin was measured in the standard assay buffer (41), which contains Mg^{++} and Ca^{++}, as well as in perfusion buffers, which contain Mg^{++}, EGTA, and no Ca^{++}. Since the effect of DNase I on streaming was determined with DNase I in TPF, it would be desirable to measure the enzyme activity in TPF as well. Interference from the large 260 nm absorbance of 1 mM ATP prevented such measurement, however, so measurements were made instead using TPF less ATP and also TPF with 0.1 mM ATP. Results are presented in Table I. Although nuclease activity fell by more than two orders of magnitude in changing from the standard buffer to TPF less ATP, the fractional inhibition of activity produced by an equimolar concentration of rabbit actin did not decrease. Use of TPF with 0.1 mM ATP as the assay buffer decreased nuclease activity by a small additional amount and reduced slightly the fractional inhibition by rabbit actin (Table I).

TABLE I

Enzyme Activities of DNase I and FL-DNase I

Enzyme and buffer	Relative nuclease activity: With no actin A	Relative nuclease activity: With equimolar rabbit actin B	Fractional inhibition (A − B)/A
DNase I			
Standard buffer	1.00	0.24	0.76
TPF less ATP	0.0027	0.00057	0.79
TPF with 0.1 mM ATP	0.0017	0.00062	0.64
FL-DNase I			
Standard buffer	0.70	0.42	0.40

All enzyme rates are expressed relative to the rate of 44 A_{260} U min^{-1} mg^{-1} for DNase I in the standard buffer of Lindberg (41).

Perfusion of Cells with Fluorescent DNase I

Enzymatic assay showed that FL-DNase I retained ~70% of the nuclease activity of the unlabeled, starting DNase I when tested under standard conditions (Table I). When assayed in the presence of an equimolar concentration of rabbit actin, the nuclease activity of FL-DNase I was inhibited 40% as compared to 76% inhibition observed with DNase I.

The ability of FL-DNase I to bind to actin in TPF was tested by incubating formaldehyde-fixed PtK_2 cells for 40 min with 0.040 mg/ml FL-DNase I in TPF. These cells showed intense staining of stress fibers and microfilaments (Fig. 3). Preincubation of FL-DNase I with a 20-fold molar excess of rabbit actin prevented staining of these structures (results not shown). Colabeling of stress fibers and microfilaments was observed when fluorescent DNase I and fluorescent phallacidin, an actin-binding mushroom toxin, were applied together to PtK_2 cells (35).

Fluorescence staining of *Chara* cells was accomplished by performing a sequence of Williamson-type perfusions (10) as described previously (31). Cells perfused for 40 min with 0.5 mg/ml FL-DNase I in TPF showed no detectable fluorescence staining of actin bundles (Fig. 4*a*) and no inhibition of cytoplasmic streaming (results not shown). When the same cells were subsequently perfused for 20 min with 0.5 mg/ml FL-HMM in TPF less ATP, intense staining of subcortical actin bundles was observed (Fig. 4*b*). As reported previously (31) for cells not exposed to DNase I, the thick layer of bound FL-HMM often permitted observation of the bundles by bright-field microscopy as well as by fluorescence microscopy (Fig. 4*c*).

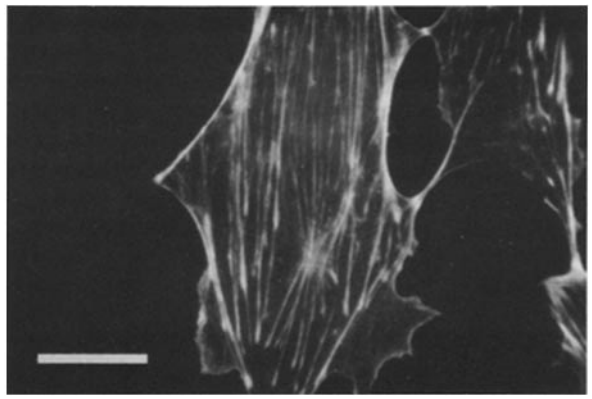

FIGURE 3 Stress fibers and microfilaments in interphase rat kangaroo (PtK_2) cells. Fluorescence micrograph showing staining after 40-min incubation with 0.040 mg/ml Fl-DNase I in TPF. Bar, 20 μm. × 730.

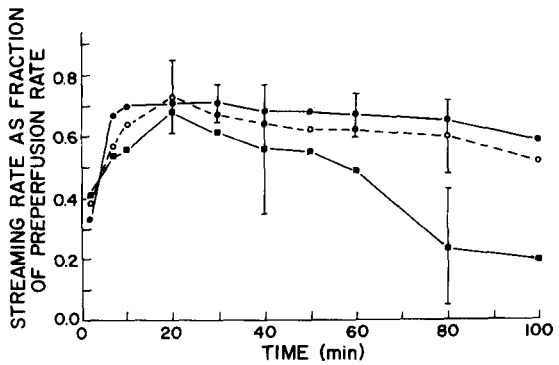

FIGURE 2 Effects on streaming of proteins applied intracellularly by Tazawa's perfusion technique. Cells were perfused with TPF (closed squares, average of seven trials), 0.5 mg/ml DNase I in TPF (open circles, average of five trials), or 0.5 mg/ml BSA in TPF (closed circles, average of four trials). Average preperfusion streaming rates were 78 (closed squares), 81 (open circles), and 93 μm/s (closed circles).

Various treatments were used in other attempts at producing FL-DNase I staining in *Chara*. These treatments included: prefixation by perfusion for 30 min with 3% formaldehyde in TPF, prestabilization by perfusion for 30 min with 1 mM phalloidin in TPF, and substitution of TPF less ATP in place of TPF in the FL-DNase I staining solution. In all cases FL-DNase I showed absolutely no detectable staining of actin bundles in *Chara*. When the same cells were subsequently perfused with FL-HMM, however, fluorescent actin bundles were readily observed (results not shown).

Effect of HMM and FL-HMM on Streaming

Preliminary experiments indicated that streaming was strongly inhibited by TPF containing FL-HMM at 0.1–0.5 mg/ml. Since TPF contains only 1 mM ATP, it seemed possible that this inhibition of streaming could have developed because all the ATP had been hydrolyzed by the added enzyme. To

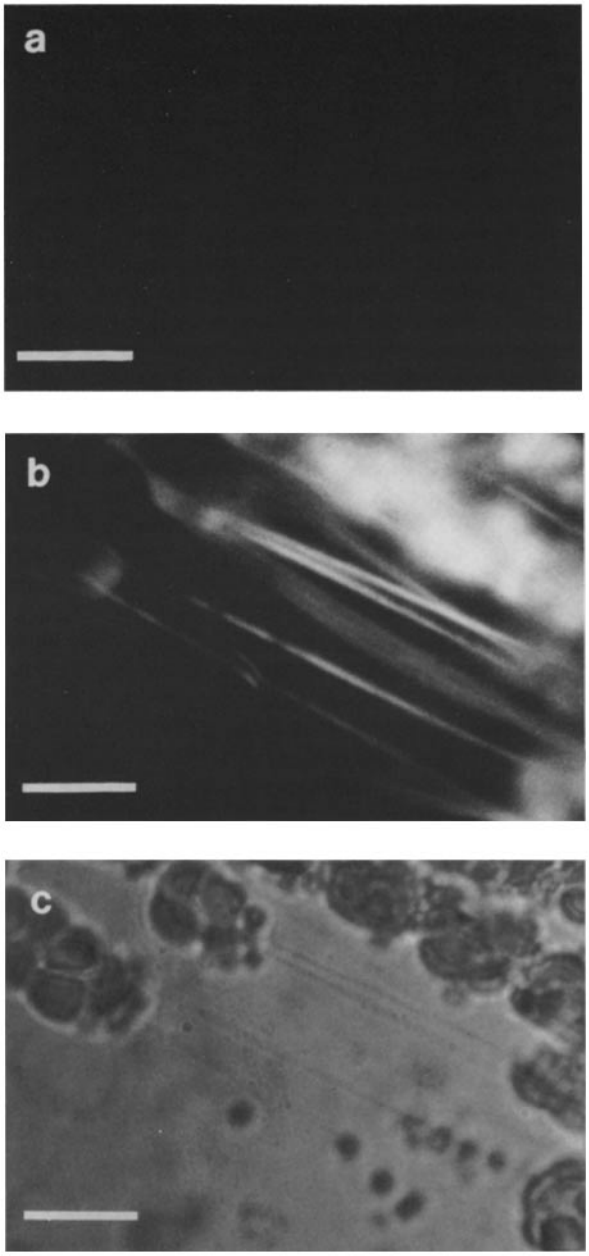

FIGURE 4 Absence of FL-DNase I staining and subsequent FL-HMM staining of actin bundles in a chloroplast window in *Chara*. Fluorescent proteins were applied by performing a sequence of Williamson-type perfusions (10, 31) that left the cell essentially devoid of endoplasm. All micrographs show the same window in the same cell. (*a*) Fluorescence micrograph recorded after 40-min perfusion with 0.5 mg/ml FL-DNase I in TPF. No fluorescence staining in any plane of focus. (*b*) Fluorescence micrograph recorded after subsequent 20-min perfusion with 0.5 mg/ml FL-HMM in TPF less ATP. (*c*) Brightfield micrograph corresponding to *b*. Bars, 10 μm. × 1,500.

circumvent this ambiguity, all subsequent experiments were conducted using TPF with 10 mM MgATP. Taking the actin-activated MgATPase activity of HMM as 0.82 μmol ATP min^{-1} mg^{-1} (29) and a HMM concentration of 0.5 mg/ml, then the time required to reduce the ATP concentration from 10 mM to 0.3 mM (0.3 mM being saturating for streaming [43]) would be ~24 min. In perfused *Chara* cells, however, the only actin available for HMM activation is in the endoplasm-ectoplasm region near the cell periphery. The MgATPase activity of unactivated HMM in the vacuolar region is an order of magnitude less than the actin-activated MgATPase and hence negligible. Some of the HMM in the vacuolar region might be activated by diffusing out to the actin bundles near the chloroplasts. Assuming a diffusion coefficient of $D = 2 \times 10^{-7}$ cm^2/s for a protein the size of HMM (44) and a cell radius of 350 μm, the characteristic time for this diffusion is $t = \overline{r^2}/(4D) =$ 26 min. Since an additional 10 min is required for the dissolution of the tonoplast at the start of the experiment, a conservative estimate for the earliest possible appearance of ATP depletion effects is 50 min after perfusion.

Perfusion of cells with TPF with 10 mM MgATP caused partial inhibition of streaming when compared to perfusion with TPF (Fig. 5; cf. Fig. 2). Streaming in TPF with 10 mM MgATP cells declined steadily from 10 min after perfusion until 40 min after perfusion at which time the streaming rate stabilized at ~20% of the preperfusion rate. Streaming in cells perfused with TPF with 10 mM MgATP also showed somewhat greater cell-to-cell variability than streaming in cells perfused with TPF. Effects of various treatments on streaming in these cells were usually clearly discernible only after data from six to nine experiments had been averaged. TPF with 10 mM MgATP also accelerated dilution of the endoplasm into the vacuolar region so that by 40 min after perfusion there frequently remained only small (~10 μm diameter) separated masses of endoplasm moving along the subcortical actin bundles.

Streaming in cells perfused with 0.5 mg/ml HMM in TPF with 10 mM MgATP was not significantly different from streaming in control cells perfused with only TPF with 10 mM MgATP (Fig. 5). Other control cells were perfused with 0.5 mg/ml ovalbumin in TPF with 10 mM MgATP. Streaming in these cells was not significantly different from streaming in either the HMM-treated cells or the TPF with 10 mM MgATP controls (Fig. 5).

When cells were perfused with 0.5 mg/ml FL-HMM in TPF with 10 mM MgATP, the streaming rate fell abruptly at 10 min and was 0 by 20 min (Fig. 6). Likewise the amount of streaming endoplasm fell sharply so that very little endoplasm remained on the ectoplasm by the time that streaming stopped at 20 min (results not shown). When the FL-HMM concentration was lowered to 0.1 mg/ml in TPF with 10 mM MgATP, inhibition of streaming was again evident at 10 min (Fig. 6). Under these conditions, however, the streaming rate declined

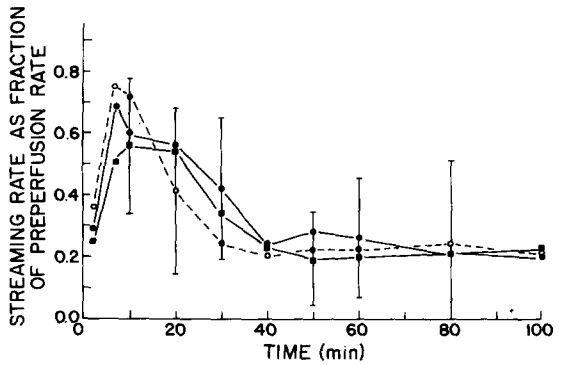

FIGURE 5 Effects on streaming of proteins applied intracellularly by Tazawa's perfusion technique. Cells were perfused with TPF with 10 mM MgATP (closed circles, average of six trials), 0.5 mg/ml HMM in TPF with 10 mM MgATP (open circles, average of nine trials), or 0.5 mg/ml ovalbumin in TPF with 10 mM MgATP (closed squares, average of eight trials). Average preperfusion streaming rates were 80 (closed circles), 80 (open circles), and 79 μm/s (closed squares).

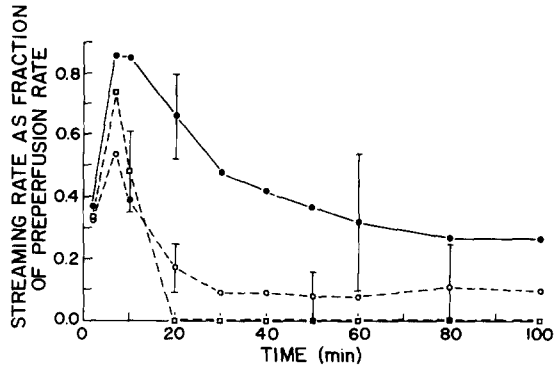

FIGURE 6 Effects on streaming of proteins applied intracellularly by Tazawa's perfusion technique. Cells were perfused with 0.1 mg/ml FL-HMM in TPF with 10 mM MgATP (open circles, average of six trials), 0.5 mg/ml FL-HMM in TPF with 10 mM MgATP (open squares, average of three trials), or 0.5 mg/ml FL-RAG in TPF with 10 mM MgATP (closed circles, average of four trials). Average preperfusion streaming rates were 81 (open circles), 70 (open squares), and 82 μm/s (closed circles).

less sharply and by 30 min had stabilized at ~10% of the preperfusion rate.

Streaming in control cells perfused with FL-RAG at 0.5 mg/ml in TPF with 10 mM MgATP declined less rapidly than streaming in cells perfused with only TPF with 10 mM MgATP (Fig. 6; cf. Fig. 5). By 100 min, however, streaming in the FL-RAG cells was only slightly faster than that in the TPF with 10 mM MgATP control.

Streaming was not inhibited when control cells were perfused with 100 μM 6-carboxyfluorescein. Even larger concentrations of fluorescein were accumulated in intact cells by incubation for 4 h with 2 μg/ml fluorescein diacetate in the extracellular medium. Streaming in these intact cells was not inhibited by the accumulated fluorescein (results not shown).

Enzymatic and Actin Binding Properties of FL-HMM

HMM and FL-HMM were partially characterized by determination of their Ca and EDTA ATPase activities. The Ca and EDTA ATPase activities (μmol ATP min^{-1} mg^{-1}) for HMM were 0.29 and 1.13, respectively. The Ca and EDTA ATPase activities for FL-HMM were 0.35 and 0.22, respectively. Hence, the Ca ATPase activities of the two proteins were similar while the EDTA ATPase activity of FL-HMM was only 20% that of HMM.

The binding of FL-HMM to actin bundles in *Chara* was tested in the absence and presence of 10 mM MgATP. FL-HMM produced intense staining of actin bundles when applied in TPF less ATP (cf. Fig. 4*b*). When applied in TPF with 10 mM MgATP, FL-HMM staining was weak and produced low density on film negatives. To quantify this difference in binding, cells were perfused continuously by the Williamson technique (10, 31) for 15 min with 0.5 mg/ml FL-HMM in TPF less ATP. At the end of this 15 min, unbound FL-HMM was removed from the cells by rapid perfusion with TPF less ATP, and then fluorescence micrographs of the stained bundles were recorded immediately. The identical experiment was performed on other cells except that FL-HMM was applied in TPF with 10 mM MgATP instead of in TPF less ATP. Negative film images of fluorescent bundles appearing in the two resulting sets of micrographs were scanned with a microdensitometer as described previously (31). The bundle profiles thus obtained were corrected for the characteristic response of the film (31), and these corrected profiles were then measured to determine integrated intensities. If an intensity of 1.0 is assigned to bundles stained in TPF less ATP, then the relative intensity for the bundles stained in TPF with 10 mM MgATP was 0.078 ± 0.058.

The amount of FL-HMM bound to subcortical actin bundles after streaming had been halted by FL-HMM was determined in a similar manner. Cells were perfused by the Tazawa technique (31, 34) with 0.5 mg/ml FL-HMM in TPF with 10 mM MgATP as had been done previously. As soon as streaming came to a full stop at ~20 min after perfusion (Fig. 6), unbound FL-HMM was quickly removed by rapid Williamson-type perfusion (10, 31) with TPF less ATP. Fluorescence micrographs of the labeled bundles were recorded and then analyzed as above. Again expressed relative to the 1.0 intensity assigned to bundles labeled in TPF less ATP, the relative intensity appearing on bundles after streaming inhibition was 0.102 ± 0.083.

DISCUSSION

Exogenous Actin Inhibits Cytoplasmic Streaming

One attractive interpretation of the inhibition of streaming by exogenous actin (Fig. 1) is that streaming inhibition occurred because the exogenous actin competitively inhibited the hypothetical force generating interaction between subcortical actin bundles and presumptive endoplasmic myosin.

Another possible interpretation is that the added actin polymerized in the endoplasm and thereby increased endoplasmic viscosity to inhibitory levels. (In these experiments the actin, tubulin, or antibody solutions were held as monomer stock solutions. Immediately before perfusion, conditions favorable for polymerization or aggregation were produced by adjustment of buffer composition or temperature, or by mixture of separate solutions). The observations (Fig. 1) that streaming was not inhibited by control perfusions with tubulin (which can also polymerize in the perfusion buffer) or mixed antibodies (which can combine to form a supramolecular aggregate) argue against a simple viscosity mechanism. Such a mechanism probably cannot be completely dismissed, however, without direct measurement of endoplasmic viscosity during the perfusions.

An earlier study (31) led to the conjecture that the concentration of free endoplasmic actin in *Chara* is normally very low and that a higher concentration would inhibit streaming. It was also hypothesized (31) that cytochalasin B (CB) may raise the endoplasmic actin concentration by releasing small amounts of actin from the subcortical bundles and thereby inhibit streaming. Fig. 1 shows that endoplasmic actin does inhibit streaming, and this data can be used to evaluate the CB hypothesis.

Data from ultrastructural studies (45, 46) on characean subcortical actin bundles can be used to estimate the amount of actin in these bundles. For a cell of diameter 0.7 mm and length 4 cm, the total amount of actin in the bundles is ~0.09 μg (47). To produce an inhibitory (Fig. 1) 0.1 mg/ml endoplasmic actin concentration, CB would have to release about half of this 0.09 μg of actin into the 10 μm thick sleeve of endoplasm in an intact cell. Loss of this much actin would thin the bundles to ~70% of their original diameter. Electron microscope studies on CB-treated cells (46) have not revealed such a significant decrease in bundle diameter. Hence for this

hypothesis on CB action to remain tenable, it is necessary to assume that *Chara* actin released by CB is, because of its molecular nature or site of release, much more potent as an inhibitor than is rabbit actin introduced by perfusion.

Exogenous DNase I Does Not Inhibit Cytoplasmic Streaming

Lack of inhibition of *Chara* streaming by DNase I (Fig. 2) contrasts with the inhibitions of *Amoeba* streaming (22) and axonal transport (23, 24) caused by microinjected DNase I. The slight stabilization of *Chara* streaming observed with DNase I was also observed with some control proteins such as BSA and antibodies but not with other controls such as tubulin and ovalbumin (Figs. 1, 2, 5, and 6). The mechanism of this streaming stabilization is not clear, but may involve a trivial effect such as protection of endogenous motile proteins against denaturation or proteolysis by endogenous enzymes.

Lack of inhibition of *Chara* streaming by DNase I cannot be readily attributed to inadequate or inactive reagent. With 0.09 μg of actin per *Chara* cell, a 100-fold molar excess of DNase I over actin was present in cells not inhibited by 0.5 mg/ml DNase I (Fig. 2). In contrast, muscle F-actin is >50% depolymerized within 20 min by an equimolar concentration of DNase I in vitro (21). Likewise, the actin-binding activity of DNase I appeared intact in the perfusion buffer as judged from the fractional inhibition of nuclease activity by rabbit actin (Table I).

Does Chara Actin Lack the DNase I Binding Site?

No staining of *Chara* actin bundles could be detected (Fig. 4*a*) when FL-DNase I was applied at >10 times the concentration used to stain stress fibers and microfilaments in PtK_2 cells (Fig. 3). While bound HMM blocks DNase I action on F-actin (21), blockage of FL-DNase I staining by *Chara* myosin is not likely because the ATP present in TPF should prevent strong myosin binding. Although profilin (48) and troponin-tropomyosin (21) do not block DNase I-actin interaction, the possibility remains that some other actin-binding protein may do so in *Chara*.

Actin from the amoeba *Naegleria gruber* does not have a strong DNase I binding site (49). Lack of streaming inhibition by DNase I in *Chara* and lack of bundle staining by FL-DNase I together suggest that *Chara* actin may also lack the usual DNase I binding site. This conjecture is intriguing because, so far, characean actin has appeared much like other actins, judging from its ability to bind skeletal muscle HMM (4, 8, 13, 31), phallotoxins (7, 31), and antibodies directed against *Physarum* (6) and human smooth muscle actins (5).

Cytoplasmic Streaming Is Inhibited by a Modified HMM

Partial inhibition of streaming in cells perfused with TPF with 10 mM MgATP (Fig. 5) compared to cells perfused with TPF (Fig. 2) is similar to high MgATP inhibition of motility in other actin-myosin-dependent systems (2, 50). The mechanism of this partial inhibition is not known but the accompanying accelerated separation of *Chara* endoplasm from the subcortical actin bundles suggests that excessive dissociation of actin-myosin may be involved.

Earlier studies have shown that HMM does not inhibit chloroplast rotation in *Nitella* endoplasmic drops (32), actin bundle movement in *Nitella* cell fragment preparations (13), stress fiber (2) or muscle fibril (29) contraction, or cell division in amphibian eggs (30). Likewise HMM did not inhibit streaming in perfused *Chara* cells (Fig. 5). Ineffectiveness of added HMM as a competitive inhibitor in these motile systems may indicate an excess of actin over myosin in the endogenous protein pools.

Perfusion of *Chara* with FL-HMM having only 20% of the EDTA ATPase expected for HMM (29, 30) resulted in abrupt inhibition of streaming (Fig. 6) and separation of endoplasm from the subcortical actin bundles. Control experiments with FL-RAG or fluorescein dyes showed that this inhibition of streaming was not a trivial effect due to the fluorescein ligand itself.

Depressed EDTA ATPase and tenacious actin binding in the presence of MgATP are properties of sulfhydryl-modified HMM (29, 30, 33). By analogy to sulfhydryl-modified HMM, the depressed EDTA ATPase of FL-HMM suggested that this FITC-modified HMM may also bind tightly to actin in the presence of MgATP.

Depressed EDTA ATPase and tenacious actin binding in the presence of MgATP are properties of sulfhydryl-modified HMM (29, 30, 33). By analogy to sulfhydryl-modified HMM, the depressed EDTA ATPase of FL-HMM suggested that this FITC-modified HMM may also bind tightly to actin in the presence of MgATP.

The association constant between HMM and F-actin has been estimated as $K_a = 3 \times 10^9\ M^{-1}$ in the absence of ATP (51) and as $K_a = 4 \times 10^3\ M^{-1}$ in the presence of millimolar MgATP (52). These association constants together with the equations of Greene and Eisenberg (51) can be used to calculate fractional saturation under conditions of specified unbound HMM concentration. Fractional saturation, θ_{HMM}, is the concentration of HMM bound to actin divided by the total concentration of actin. If the concentration of unbound HMM is taken as 1.4×10^{-6} M (0.5 mg/ml), then the result is $\theta_{HMM} = 0.00551$ in the presence of millimolar MgATP, and $\theta_{HMM} = 0.496$ in the absence of MgATP. If FL-HMM binds like HMM, then the ratio of these fractional saturations, 0.00551/0.496 = 0.0111, should be the same as the ratio of bundle staining with 0.5 mg/ml FL-HMM in the presence and absence of MgATP. This ratio was measured as 0.078 ± 0.058.

Although MgATP greatly reduced the binding between FL-HMM and *Chara* actin bundles, the calculation above suggests that this binding was still about seven times stronger than that expected for HMM. This calculation assumes that binding constants measured between rabbit HMM and rabbit actin are also accurate for rabbit HMM and *Chara* actin. If this assumption is valid, then it appears that inhibition of *Chara* streaming by FL-HMM, but not by HMM, may have occurred because FL-HMM bound to and blocked the actin bundles even in the presence of MgATP.

The amount of FL-HMM bound to the bundles at the time of inhibition, expressed relative to the amount bound in TPF less ATP, was measured as 0.102 ± 0.083. The fractional saturation for binding in the absence of ATP was $\theta_{HMM} = 0.496$, and scaling this number by the measured fluorescence ratio of 0.102 gives $\theta_{HMM} = 0.051$ at the time of inhibition. Allowing for the binding of each FL-HMM to two actins (51), this result indicates that streaming was fully inhibited when only 10% of the accessible actins were found to FL-HMM.

Conclusions

The major conclusions of this study are: (*a*) Exogenous actin is a potent inhibitor of cytoplasmic streaming. (*b*) DNase I does not inhibit streaming, and FL-DNase I does not bind to *Chara* actin bundles. *Chara* actin apparently lacks the DNase I binding site. (*c*) HMM does not inhibit streaming but FL-HMM having a partially inactive EDTA ATPase does. (*d*) FL-HMM may inhibit streaming by binding to the subcortical actin bundles even in the presence of MgATP. These results support the hypothesis that cytoplasmic streaming in *Chara* is generated by interaction between subcortical actin bundles and presumptive endoplasmic myosin.

We are indebted to Stuart J. Edelstein and Bruce McEwen for their gift of tubulin and to Roger M. Spanswick for supplying us with starting cultures of *Chara*. We thank Larry S. Barak for preparing the PtK_2 cells and Masashi Tazawa for demonstrating his perfusion technique.

Support was provided by a National Institutes of Health (NIH) predoctoral traineeship (GM07273 to E. A. Nothnagel), grants to W. W. Webb (NIH, GM21661 and National Science Foundation, PCM8007637), to J. W. Sanger (NIH, GM25653 and HL15835), and use of facilities of the Materials Science Center at Cornell.

Received for publication 7 May 1981, and in revised form 26 October 1981.

REFERENCES

1. Clarke, M., and J. A. Spudich. 1977. Nonmuscle contractile proteins: the role of actin and myosin in cell motility and shape determination. *Annu. Rev. Biochem.* 46:797–822.
2. Kreis, T. E., and W. Birchmeier. 1980. Stress fiber sarcomeres of fibroblasts are contractile. *Cell.* 22:555–561.
3. Allen, N. S., and R. D. Allen. 1978. Cytoplasmic streaming in green plants. *Annu. Rev. Biophys. Bioeng.* 7:497–526.
4. Palevitz, B. A., and P. K. Hepler. 1975. Identification of actin *in situ* at the ectoplasm-endoplasm interface of *Nitella*. *J. Cell Biol.* 65:29–38.
5. Williamson, R. E., and B. H. Toh. 1979. Motile models of plant cells and the immunofluorescent localization of actin in a motile *Chara* cell model. *In* Cell Motility: Molecules and Organization. S. Hatano, H. Ishikawa, and H. Sato, editors. University of Tokyo Press, Tokyo. 339–346.
6. Hatano, S., K. Owaribe, F. Matsumura, T. Hasegawa, and S. Takahashi. 1980. Characterization of actin, actinin, and myosin isolated from *Physarum*. *Can. J. Bot.* 58:750–759.
7. Barak, L. S., R. R. Yocum, E. A. Nothnagel, and W. W. Webb. 1980. Fluorescence staining of the actin cytoskeleton in living cells with nitrobenzoxadiazole-phallacidin. *Proc. Natl. Acad. Sci. U. S. A.* 77:980–984.
8. Kersey, Y. M., P. K. Hepler, B. A. Palevitz, and N. K. Wessells. 1976. Polarity of actin filaments in characean algae. *Proc. Natl. Acad. Sci. U. S. A.* 73:165–167.
9. Kamiya, N., and K. Kuroda. 1956. Velocity distribution of the protoplasmic streaming in *Nitella* cells. *Bot. Mag. Tokyo.* 69:544–554.
10. Williamson, R. E. 1975. Cytoplasmic streaming in *Chara*: a cell model activated by ATP and inhibited by cytochalasin B. *J. Cell Sci.* 17:655–668.
11. Kamitsubo, E. 1972. Motile protoplasmic fibrils in cells of the *Characeae*. *Protoplasma (Berl.).* 74:53–70.
12. Jarosch, R. 1957. Zur Mechanik der Protoplasmafibrillen-bewegung. *Biochim. Biophys. Acta.* 25:204–205.
13. Higashi-Fujime, S. 1980. Active movement in vitro of bundles of microfilaments isolated from *Nitella* cell. *J. Cell Biol.* 87:569–578.
14. Kato, T., and Y. Tonomura. 1977. Identification of myosin in *Nitella flexilis*. *J. Biochem. (Tokyo).* 82:777–782.
15. Williamson, R. E. 1979. Filaments associated with the endoplasmic reticulum in the streaming cytoplasm of *Chara corallina*. *Eur. J. Cell Biol.* 20:177–183.
16. Nagai, R., and T. Hayama. 1979. Ultrastructure of the endoplasmic factor responsible for cytoplasmic streaming in *Chara* internodal cells. *J. Cell Sci.* 36:121–136.
17. Allen, N. S. 1980. Cytoplasmic streaming and transport in the characean alga *Nitella*. *Can. J. Bot.* 58:786–796.
18. Mabuchi, I., and M. Okuno. 1977. The effect of myosin antibody on the division of starfish blastomeres. *J. Cell Biol.* 74:251–263.
19. Asai, D. J., and C. J. Brokaw. 1980. Effects of antibodies against tubulin on the movement of reactivated sea urchin sperm flagella. *J. Cell Biol.* 87:114–123.
20. Gibbons, B. H., K. Ogawa, and I. R. Gibbons. 1976. The effect of antidynein 1 serum on the movement of reactivated sea urchin sperm. *J. Cell Biol.* 71:823–831.
21. Hitchcock, S. E., L. Carlsson, and U. Lindberg. 1976. DNase I-induced depolymerization of actin filaments. *Cold Spring Harbor Conf. Cell Proliferation.* 3(Book B):545–559.
22. Wehland, J., K. Weber, W. Gawlitta, and W. Stockem. 1979. Effects of the actin-binding protein DNAase I on cytoplasmic streaming and ultrastructure of *Amoeba proteus*. *Cell Tissue Res.* 199:353–372.
23. Isenberg, G., P. Schubert, and G. W. Kreutzberg. 1980. Experimental approach to test the role of actin in axonal transport. *Brain Res.* 194:588–593.
24. Goldberg, D. J., D. A. Harris, B. W. Lubit, and J. H. Schwartz. 1980. Analysis of the mechanism of fast axonal transport by intracellular injection of potentially inhibitory macromolecules: evidence for a possible role of actin filaments. *Proc. Natl. Acad. Sci. U. S. A.* 77:7448–7452.
25. Wang, Y. L., and D. L. Taylor. 1979. Distribution of fluorescently labeled actin in living sea urchin eggs during early development. *J. Cell Biol.* 82:672–679.
26. Sanger, J. W., J. M. Sanger, T. E. Kreis, and B. M. Jockusch. 1980. Reversible translocation of cytoplasmic actin into the nucleus caused by dimethyl sulfoxide. *Proc. Natl. Acad. Sci. U. S. A.* 77:5268–5272.
27. Taylor, D. L., and Y. L. Wang. 1980. Fluorescently labelled molecules as probes of the structure and function of living cells. *Nature (Lond.)* 284:405–410.
28. Wang, Y. L., and D. L. Taylor. 1980. Preparation and characterization of a new cytochemical probe: 5-iodoacetamidofluorescein-labeled actin. *J. Histochem. Cytochem.* 28:1198–1206.
29. Meeusen, R. L., and W. Z. Cande. 1979. N-Ethylmaleimide-modified heavy meromyosin: a probe for actomyosin interactions. *J. Cell Biol.* 82:57–65.
30. Meeusen, R. L., J. Bennett, and W. Z. Cande. 1980. Effect of microinjected N-ethylmaleimide-modified heavy meromyosin on cell division in amphibian eggs. *J. Cell Biol.* 86:858–865.
31. Nothnagel, E. A., L. S. Barak, J. W. Sanger, and W. W. Webb. 1981. Fluorescence studies on modes of cytochalasin B and phallotoxin action on cytoplasmic streaming in *Chara*. *J. Cell Biol.* 88:364–372.
32. Kuroda, K., and N. Kamiya. 1975. Active movement of *Nitella* chloroplasts *in vitro*. *Proc. Jpn. Acad.* 51:774–777.
33. Ishiura, M., K. Shibata-Sekiya, T. Kato, and Y. Tonomura. 1977. A chemically modified subfragment-1 of myosin from skeletal muscle as a novel tool for identifying the function of actomysin in non-muscle cells. *J. Biochem. (Tokyo).* 82:105–115.
34. Tazawa, M., M. Kikuyama, and T. Shimmen. 1976. Electrical characteristics and cytoplasmic streaming of characean cells lacking tonoplast. *Cell Struct. Funct.* 1:165–176.
35. Barak, L. S., E. A. Nothnagel, E. F. DeMarco, and W. W. Webb. 1981. Differential staining of actin in metaphase spindles with NBD-phallacidin and fluorescent deoxyribonuclease: is actin involved in chromosomal movement? *Proc. Natl. Acad. Sci. U. S. A.* 78:3034–3038.
36. Crepeau, R. H., B. McEwen, G. Dykes, and S. J. Edelstein. 1977. Structural studies on porcine brain tubulin in extended sheets. *J. Mol. Biol.* 116:301–315.
37. Wharton, D. C., and R. E. McCarty. 1972. Experiments and Methods in Biochemistry. Macmillan Publishing Co., Inc., New York.
38. Spudich, J. A., and S. Watt. 1971. The regulation of rabbit skeletal muscle contraction. *J. Biol. Chem.* 246:4866–4871.
39. Sanger, J. W. 1975. Changing patterns of actin localization during cell division. *Proc. Natl. Acad. Sci. U. S. A.* 72:1913–1916.
40. Wang, E., and A. R. Goldberg. 1978. Binding of deoxyribonuclease I to actin: a new way to visualize microfilament bundles in non-muscle cells. *J. Histochem. Cytochem.* 26:745–749.
41. Lindberg, U. 1964. Purification of an inhibitor of pancreatic deoxyribonuclease from calf spleen. *Biochim. Biophys. Acta.* 82:237–248.
42. Lazarides, E., and U. Lindberg. 1974. Actin is the naturally occurring inhibitor of deoxyribonuclease I. *Proc. Natl. Acad. Sci. U. S. A.* 71:4742–4746.
43. Shimmen, T. 1978. Dependency of cytoplasmic streaming on intracellular ATP and Mg^{++} concentrations. *Cell Struct. Funct.* 3:113–121.
44. Diem, K., and C. Lenter. 1970. Scientific Tables. 7th ed. Ciba-Geigy Ltd., Basle, Switzerland.
45. Nagai, R., and L. I. Rebhun. 1966. Cytoplasmic microfilaments in streaming *Nitella* cells. *J. Ultrastruct. Res.* 14:571–589.
46. Bradley, M. O. 1973. Microfilaments and cytoplasmic streaming: inhibition of streaming with cytochalasin. *J. Cell Sci.* 12:327–343.
47. Nothnagel, E. A. 1981. Studies on the mechanism of cytoplasmic streaming in *Chara corallina*. PhD thesis. Cornell University.
48. Korn, E. D. 1978. Biochemistry of actomyosin-dependent cell motility. *Proc. Natl. Acad. Sci. U. S. A.* 75:588–599.
49. Sussman, D. J., E. Y. Lai, and C. Fulton. 1980. Unusual features of *Naegleria* actin. *J. Cell Biol.* 87(2, Pt. 2):223*a* (Abstr.).
50. Cande, W. Z. 1980. A permeabilized cell model for studying cytokinesis using mammalian tissue culture cells. *J. Cell Biol.* 87:326–335.
51. Greene, L. E., and E. Eisenberg. 1980. The binding of heavy meromyosin to F-actin. *J. Biol. Chem.* 255:549–554.
52. Eisenberg, E., and C. Moos. 1968. The adenosine triphosphatase activity of acto-heavy meromyosin: a kinetic analysis of actin activation. *Biochemistry* 7:1486–1489.